Journal of Hazardous Materials 489 (2025) 137702

Contents lists available at ScienceDirect

Journal of Hazardous Materials

journal homepage: www.elsevier.com/locate/jhazmat

Variable dual C-Cl isotope slopes of trichloromethane transformation by alkaline-activated persulfate under different simulated field conditions

Sergio Gil-Villalba [a,*], Mònica Rosell [a], Clara Torrentó [a,b], Martí Vinyes-Nadal [a], Albert Soler [a], Jordi Palau [a]

[a] Grup MAiMA, SGR Mineralogia Aplicada, Geoquímica i Hidrogeologia (MAGH), Departament de Mineralogia, Petrologia i Geologia Aplicada, Facultat de Ciències de la Terra, Institut de Recerca de l'Aigua (IdRA), Universitat de Barcelona (UB), Martí Franquès s/n, Barcelona 08028, Spain
[b] Serra Húnter Fellowship, Generalitat de Catalunya, Spain

HIGHLIGHTS

- TCM:PS molar ratio influences oxidation kinetics, but not isotopic fractionation.
- Alkaline hydrolysis becomes predominant at pHs higher than 12.
- The presence of carbonates points to a reductive degradation reaction.
- Dual C-Cl isotope analysis allowed the identification of the different reactions.
- Hexachloroethane was observed as degradation byproduct.

GRAPHICAL ABSTRACT

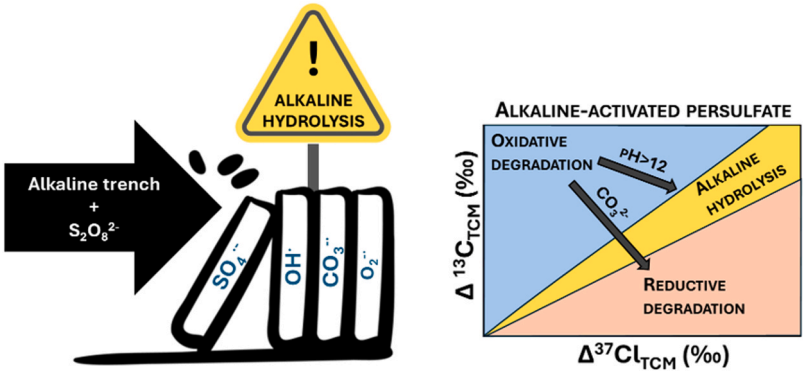

ARTICLE INFO

Keywords:
2D-CSIA
Chloroform
Advanced oxidation treatments
In situ chemical oxidation
Groundwater remediation
Chlorinated contaminants

ABSTRACT

Laboratory experiments were conducted to evaluate the potential of $\delta^{13}C$ and $\delta^{37}Cl$ isotopic values of trichloromethane (TCM) to monitor and quantify its transformation during alkaline persulfate (PS) activation. Batch experiments were designed to replicate different TCM:PS molar ratios, pH values, the presence of CO_3^{2-} ion and the simulation of an alkaline interception trench. Results revealed three distinct C-Cl isotopic trends; First, despite differences in degradation kinetics, isotopic trends were consistent across TCM:PS molar ratios (Λ^{C-Cl} between 23 ± 10 and 33 ± 6), suggesting that radical activation remained unaffected. Conversely, at pH 12.8, alkaline hydrolysis (AH) became the predominant degradation process (Λ^{C-Cl} of 9 ± 1 and 11 ± 1) over reaction with PS derived radical species. Finally, in the presence of excess CO_3^{2-} ion, which acts as radical scavenger probably affecting the radical species involved in TCM degradation, a Λ^{C-Cl} value of 5.5 ± 0.6 was observed, suggesting a reductive degradation reaction. Therefore, our results reveal, for the first time, that the dual C-Cl isotope slope during TCM degradation by PS varies significantly depending on field conditions. The unexpected accumulation of higher chlorinated byproducts, such as hexachloroethane, during TCM degradation by alkaline-

* Corresponding author.
E-mail address: sergiogilv@ub.edu (S. Gil-Villalba).

https://doi.org/10.1016/j.jhazmat.2025.137702
Received 3 December 2024; Received in revised form 10 February 2025; Accepted 19 February 2025
Available online 22 February 2025

activated PS was observed for the first time and further research is needed in real open-systems to assess its potential environmental implications.

1. Introduction

Trichloromethane (TCM), commonly known as chloroform ($CHCl_3$), has had multiple industrial applications, and is today one of the most prevalent groundwater contaminants. TCM is a deemed toxic pollutant and, thus, it is ranked 11th in the Priority List of Hazardous Substances in 2022 by the Agency for Toxic Substances and Disease Registry based on a combination of its frequency, toxicity, and potential for human exposure [1].

In situ Chemical Oxidation (ISCO) is considered as an effective treatment method for the remediation of organic contaminants, including TCM [2-5]. Among different oxidants, activated persulfate ($S_2O_8^{2-}$, PS) has been increasingly applied in ISCO treatments of contaminated soil and groundwater due to its capacity to generate sulfate radicals ($SO_4^{\cdot-}$), which are as reactive as the classically used hydroxyl radicals ($OH^{\cdot}$), but more selective [6,7,4]. Furthermore, activated PS exhibits both oxidative and nucleophilic reactivity, leading to the generation of various reactive oxygen species (ROS) besides sulfate radicals ($SO_4^{\cdot-}$), such as $OH^{\cdot}$ and superoxide radicals ($O_2^{\cdot-}$), facilitating the degradation of multiple contaminants [8-10].

Base activation of PS, widely applied in field treatments [10], generates sulfate radicals ($SO_4^{\cdot-}$) that lead to hydroxyl radical formation ($OH^{\cdot}$) under highly alkaline conditions [11-13]. While both ROS can effectively degrade persistent organic compounds, the lower selectivity of $OH^{\cdot}$ may increase its consumption by natural organic matter, reducing treatment efficiency [8,14,15]. Furthermore, common groundwater anions like HCO_3^-, CO_3^{2-} and Cl^- can act as $SO_4^{\cdot-}$ and $OH^{\cdot}$ scavengers [14, 16,17], forming weaker oxidant radicals such as $CO_3^{\cdot-}$ and $Cl^{\cdot}$ [18-20]. These secondary radicals, while very selective, typically reduce overall oxidation kinetics and alter degradation pathways [14,21].

Therefore, in alkaline-activated PS systems, multiple degradation pathways of contaminants can coexist due to the presence of various ROS and/or the occurrence of alkaline hydrolysis [22,23]. Assessing degradation reaction mechanisms of TCM following an alkaline-activated PS application is crucial for evaluating contaminated site remediation; however, this area remains largely unexplored. Dual-element compound specific isotope analysis (2D-CSIA) offers a promising approach for distinguishing reaction mechanisms by leveraging the characteristic stable isotope fractionation patterns associated with specific degradation processes [24-27]. Given that different ROS might induce distinct TCM degradation mechanisms and that multiple degradation pathways may occur simultaneously, 2D-CSIA could provide valuable insights into the processes driving TCM transformation by alkaline-activated PS under varying environmental conditions.

Several dual C-Cl slope values (i.e., $\Lambda^{C\text{-}Cl}$) for TCM transformation processes have been previously reported. Regarding reductive processes, TCM degradation with cast zero valent iron, Fe(0), yields a $\Lambda^{C\text{-}Cl}$ value of 8 ± 2 at pH 7 [28] that remains unchanged at pH 12 [29], although it has also been reported as $\Lambda^{C\text{-}Cl} = 5.8 \pm 0.4$ [30]. TCM bacterial reductive dechlorination (RD) has been studied abiotically through the use of the corrinoid cofactor vitamin B12 (present in almost all reductive dehalogenases identified to date), obtaining a $\Lambda^{C\text{-}Cl} = 6.5 \pm 0.2$ [31]. When smaller doses of vitamin B12 were used to biostimulate anoxic microbial cultures, similar values (7 ± 1) were observed [32]. A recent work [33] attributed the reactivity of TCM with vitamin B12 by *Dehalobacter* CF (strain UNSWDHB) (with a $\Lambda^{C\text{-}Cl} = 6.6 \pm 0.1$) to a second-order nucleophilic substitution (S_N2) reaction. However, experiments using *Dehalobacter strain* 8 M exhibited a very different $\Lambda^{C\text{-}Cl}$ value of 2.8 ± 0.3, which was ascribed to enzyme binding masking effects created by the structure of different enzymatic pockets [34]. A different TCM reductive mechanism, concerted dissociative Outer-Sphere Single Electron Transfer (OS-SET), was studied by experiments with $CO_2^{\cdot-}$ radical [35], which produced a SET to a σ* orbital concerted with C-Cl breakage, leading to a similar $\Lambda^{C\text{-}Cl} = 6.7 \pm 0.4$. These reported $\Lambda^{C\text{-}Cl}$ values for reductive processes are in general lower compared to those observed for TCM alkaline hydrolysis (AH) ($\Lambda^{C\text{-}Cl} = 13.0 \pm 0.8$) and oxidation by thermally activated PS ($\Lambda^{C\text{-}Cl} = 17 \pm 2$) [28]. This is consistent with an oxidative C-H bond cleavage by a hydrogen atom abstraction (HAA) in the case of the heat-activated PS oxidation and a stepwise $E1_{CB}$ elimination reaction, consisting of the base-catalyzed deprotonation of the TCM followed by the loss of a chloride ion, for AH degradation mechanism [23].

In the light of the above information, the alkaline activation of PS in ISCO treatments could be influenced by varying field conditions, potentially resulting in the formation of different ROS or triggering processes such as alkaline hydrolysis. In turn, these variations can significantly affect the degradation pathways and overall efficiency of TCM remediation. To the best of the authors knowledge, the TCM degradation reaction mechanisms following ISCO with alkaline-activated PS have not been previously investigated. Since prior research has demonstrated that C-Cl 2D-CSIA is a valuable tool for distinguishing among different TCM degradation processes (e.g., reductive degradation, alkaline hydrolysis, and thermal-activated PS oxidation), this study aims to evaluate the potential of 2D-CSIA for assessing TCM degradation processes under variable field conditions during alkaline-activated persulfate ISCO treatments.

To this end, ISCO by alkaline-activated PS was replicated in batch experiments under controlled laboratory conditions where the influence of different factors was assessed: TCM:PS molar ratios, pH, and the presence of radical-scavenger species commonly found in groundwater (e.g., CO_3^{2-}). In addition, the novel remediation conditions provided by an interception alkaline trench filled with concrete-based residues (such the one previously studied in Òdena, Spain [23]) and multiple contaminants (i.e., chlorinated methanes - CMs and chlorinated ethenes - CEs) typically found in contaminated sites were considered. Most of the factors evaluated in this study are common in field applications of alkaline activated PS, including the use of a commercial mixed reagent.

2. Methodology

A list of all chemicals used in the laboratory experiments is provided in Appendix A in the Supplementary Information (SI).

2.1. Experimental design

Batch experiments were performed to assess the TCM carbon and chlorine isotopic fractionation during its transformation by alkaline-activated PS under different conditions (see summary in Table 1). Both commercial persulfate with an integrated alkaline activator (PersulfOx®, from now on "PSOX") and pure sodium persulfate ("PS") were used in different experiments consisting of: (i) deionized water with PSOX (resulting in a pH of 10.2 ± 0.2) with two different TCM:PS molar ratios (1:125 and 1:65), to assess the feasibility of TCM oxidation at different PSOX dosages or in different parts of a contamination plume; (ii) deionized water with PS basified with NaOH at two different alkaline pHs (11.4 ± 0.4 and 12.83 ± 0.03), to assess if changes in pH could induce changes in the oxidation reaction, other than a greater extent of AH; (iii) deionized water with PS basified as in experiment ii but adding Na_2CO_3 (at 200 mg/L), to resemble groundwater conditions and to evaluate the effect of CO_3^{2-} anion in the radical cascade activity; and (iv) trench-sampled water (pH 10.3 ± 0.5), co-contaminants (either CMs or

Table 1
Summary of experiments conditions: pH, TCM:PS molar ratio, contaminants in the aqueous solution and measured initial CO_3^{2-} concentrations.

Code	Conditions	pH	Molar ratio TCM:PS	Contaminants	Initial CO_3^{2-} (mg/L)
i.a	PSOX	10.2 ± 0.2	1:65	TCM	0
i.b	PSOX	10.2 ± 0.2	1:125	TCM	0
ii.a	PS + NaOH	11.4 ± 0.4	1:65	TCM	0
ii.b	PS + NaOH	12.8 ± 0.1	1:65	TCM	0
iii.a	PS + NaOH + CO_3^{2-}	11.3 ± 0.4	1:65	TCM	110
iii.b	PS + NaOH + CO_3^{2-}	12.8 ± 0.1	1:65	TCM	110
iv.a	PS + Trench conditions	11.6 ± 0.7	1:65	TCM, CT, DCM	95
iv.b	PS + Trench conditions	11.7 ± 0.6	-	PCE, TCE, cis-DCE	95

CEs) and filling material, plus PS to reproduce the field conditions of an alkaline interception trench.

In the last set-up (exp. iv), solid samples from an active alkaline interception trench, composed of 40–70 mm-sized recycled concrete-based aggregates from a construction waste recycling plant [23] were grinded to a diameter between 2 and 8 mm and 25 g were introduced in each vial. This experiment simulated the possible interactions of the solid phases in the oxidation reaction, while maintaining the alkaline pH for PS activation via equilibrium with the portlandite ($Ca(OH)_2$) present in the concrete. With this set-up, to reproduce the oxidation reaction in the mentioned alkaline trench, and to assess the potential of 2D-CSIA to identify the underlying oxidation process and quantify the extent of the degradation, two batch experiments were conducted, one containing CMs (tetrachloromethane - CT, TCM and dichloromethane - DCM) and another one with CEs (tetrachloroethene - PCE, trichloroethene - TCE, cis-dichloroethene - cis-DCE). For the preparation of the experiments, trench-sampled water was purged with N_2 gas for 8 hours to eliminate all volatile organic compounds present at the field site. After purging, a known concentration of the target compounds (either CMs or CEs), with a known initial isotopic composition, was added.

Additionally, control vials prepared in the same conditions as the experimental ones but without PS were analyzed to account for the extent of AH in experiments i, ii and iv.

Batch experiments were prepared filling 40 mL EPA VOA glass vials with a mixture of PS or PSOX and TCM or CMs or CEs stock solutions to reach pre-established concentrations. The vials were filled without headspace to avoid partitioning of TCM/CMs/CEs between the aqueous and gas phases and were closed with PTFE-lined caps. The experiments were conducted at 23°C in the dark in a thermostatic chamber.

The oxidation reaction was stopped after different reaction times by replacing 7.5 mL of the experimental solution with a 1.5 M ascorbic acid (AA) solution, resulting in a molar ratio of AA:PS equal to 4:1, inducing a rapid dissociation of the PS [36]. At this molar ratio, any radical reacts rapidly with the AA, inhibiting further TCM degradation [36,37]. In experiment iv, the solution was previously filtered using a 0.45 µm nylon filter to separate the solid phase from the liquid samples, before the quenching procedure with AA. The 7.5 mL aliquots extracted from the experimental vials were used to measure the pH of the experiment with a pH probe (WTW pH SenTix pH 940 electrode). Duplicate samples were always collected for each reaction time and stored at 4°C in darkness until analysis.

2.2. Analytical methods

A detailed description of the analytical methods and equipment used for concentration and isotope ratio measurements is available in Appendix B. Briefly, CEs and CMs concentrations were measured by headspace gas chromatography-mass spectrometry (HS-GC-MS) as explained elsewhere [28]. Carbon isotope analysis was performed using a GC coupled to an Isotope Ratio Mass Spectrometer (GC-IRMS) at the Technological Centers of the University of Barcelona (CCiT-UB). Chlorine isotope analysis of CT, TCM, DCM, PCE and TCE was performed by GC-qMS at the CCiT-UB using the methodology described by [38], while cis-DCE was analyzed using a GC-IRMS at Isotope Tracer Technologies Inc. (Waterloo, Canada) as described in [39]. All samples were analyzed in duplicate and corrected for slight isotopic fractionation induced by the preconcentration technique (solid-phase micro extraction – SPME) relative to daily aqueous isotopic standards of the target compounds with known isotopic composition. These aqueous isotopic standards were prepared as the samples and measured in the same sequence. Precision (1σ) of the analysis was ≤ 0.5 ‰ for $\delta^{13}C$ on all compounds and ≤ 0.2 ‰ for $\delta^{37}Cl$ of cis-DCE, and ≤ 0.5 ‰ for $\delta^{37}Cl$ of PCE, TCE and the CMs. The presence of volatile byproducts generated in the degradation process was determined using the HS-GC-qMS system in the CCiT-UB, using the previously described configuration but in full scan mode.

2.3. Isotope data evaluation

The carbon and chlorine isotopic compositions are reported in delta notation (δ^hE, in ‰, Eq. 1), relative to the international standards VPDB (Vienna Pee Dee Belemnite) and SMOC (Standard Mean Ocean Chlorine) [40,41], respectively. The isotopic ratio of a sample and the standard of an element (E) (e.g., $^{13}C/^{12}C$, $^{37}Cl/^{35}Cl$) is denoted as R_{sample} and R_{std}, respectively:

$$\delta^h E = \left(\frac{R_{sample}}{R_{std}} - 1\right) \quad (1)$$

A simplified version of the Rayleigh equation in logarithmic form (Eq. 2) can be used to correlate changes in the isotopic composition of an element in a compound (R_t / R_0) with changes in its concentration for a given reaction ($f = C_t / C_0$), by using the corresponding isotopic fractionation (ε) [24,42]:

$$\ln\left(\frac{R_t}{R_0}\right) = \varepsilon \cdot \ln(f) \quad (2)$$

where R_t / R_0 can be expressed as $(\delta^hE_t + 1) / (\delta^hE_0 + 1)$ according to the δ^hE definition. For degradation to be considered significant, differences in isotope values in the field for both carbon and chlorine must be > 2 ‰ [43].

Finally, $\Lambda^{C\text{-}Cl}$ values for specific reactions can be defined under controlled laboratory conditions. The slope of the ordinary linear regression (OLR) in the dual C-Cl isotope plot [24] with uncertainty reported as the 95 % confidence interval (CI) is calculated. Since recent studies by [44,45] suggested using the York regression method instead of OLR to determine Λ and its uncertainty, a comparison between both approaches is also shown.

Statistical differences with previously reported values for the estimated isotope fractionation values (εCl and εC) and dual isotope slopes ($\Lambda^{C/Cl}$) were assessed using statistical two-tailed z-score tests [44,45]. Differences were considered statistically significant at the $\alpha = 0.05$ confidence level.

3. Results and discussion

3.1. Experiment i: effect of TCM:PS molar ratio

The commercial product PSOX used in experiment i kept the pH at 10.2 ± 0.2, independently of the used TCM:PS molar ratio. At this pH, the primary radicals driving the oxidation are expected to be $SO_4^{\cdot-}$ and $OH^{\cdot}$ [12,13]. Degradation of TCM was observed over time, reaching 98 % after 30 days at the molar ratio of 1:65 (experiment i.a, Table 1) and after 13 days at the molar ratio of 1:125 (i.b). In the control vials, the concentration of TCM remained unchanged for up to 35 days (see

Figure C.1 in Appendix C), discarding TCM degradation by AH and ruling out potential TCM losses due to other processes such as volatilization through the caps. Therefore, TCM degradation was attributed solely to chemical oxidation, which followed pseudo-first-order kinetics, as evidenced by the good linear correlation between $\ln(C/C_0)$ and time (Figure C.1). The results show that the rate of TCM degradation increases with higher relative PS concentrations, with pseudo-first-order rate constant (k'obs) values of 0.151 and 0.232 d^{-1} (Table 2), corresponding to half-lives of 4.6 and 3.0 days for TCM:PS molar ratios of 1:65 and 1:125, respectively.

Despite these differences in TCM:PS molar ratios and degradation rates, experiments i.a and i.b exhibited comparable enrichment in ^{13}C and ^{37}Cl, while isotopic changes in the controls were not statistically significant ($p > 0.05$) (Figures C.2 and C.3). The calculated εC values were -12 ± 1 and -11 ± 1 ‰, while for chlorine the obtained εCl values were much lower, -0.30 ± 0.05 and -0.4 ± 0.2 ‰, for experiments i.a and i.b, respectively (see Table 2 for all calculated εC, εCl and $\Lambda^{C\text{-}Cl}$ values). Since no systematic bias introduced by OLR was observed compared to York method [44,45], we used OLR values, but present York results in the SI (Appendix D). The determined $\Lambda^{C\text{-}Cl}$ values did not show a significant difference either ($p > 0.05$), being 33 ± 6 and 23 ± 10 for experiments i.a and i.b, respectively. Due to the notably higher carbon isotope fractionation compared to chlorine, both $\Lambda^{C\text{-}Cl}$ values exceeded any previously reported in the literature for TCM, showing that TCM oxidation by alkaline-activated PS at this pH (10.2) can be distinguishable from other degradation processes using 2D isotopic tools.

3.2. Experiment ii: effect of pH increase

Experiments ii.a and ii.b were conducted at pH 11.4 and 12.8, respectively, where both $SO_4^{\cdot-}$ and $OH^{\cdot}$ radicals were supposed to be present [46]. An important reduction in TCM concentration was observed over time, reaching degradation percentages of 92 % after 20 days in experiment ii.a and 98 % after 67 days in experiment ii.b. Interestingly, control experiments without PS also exhibited noticeable TCM degradation within the same time period, attributed to AH. In control ii.a (pH=11.4), a 10 % reduction in TCM was observed over 20 days, while in control ii.b (pH=12.8), TCM concentration decreased by 50 % after 30 days, reaching 87 % degradation after 78 days (Figure C.1). TCM degradation, under stronger alkaline conditions than experiment i, followed pseudo-first order kinetics in both the experimental and control vials (Table 2 and Figure C.1). The observed k'obs values were 0.12 ± 0.02 and 0.053 ± 0.009 d^{-1} for experiments ii.a and ii.b, and 0.006 ± 0.003 and 0.026 ± 0.001 d^{-1} for the corresponding controls (Table 2). These results indicated that the rate of TCM degradation decreases with increasing pH. This is likely due to the predominance of AH, which has significantly slower kinetics compared to oxidation. This hypothesis is further discussed below using the isotope data.

Isotopic analysis of experiments ii.a and ii.b revealed different εC values of -10.1 ± 0.7 and -25 ± 12 ‰, and also distinct εCl values of -0.40 ± 0.1 and -2.7 ± 0.3 ‰, respectively (Table 2), leading to $\Lambda^{C\text{-}Cl}$ values of 23 ± 7 and 9 ± 2, respectively. In contrast, control ii.b showed much higher carbon and chlorine isotopic fractionation values of εC = -59 ± 16 ‰ and εCl = -5 ± 2 ‰, with a $\Lambda^{C\text{-}Cl}$ value of 11 ± 1. The latter values are consistent with those reported for TCM degradation via AH [23,28]. Carbon and chlorine isotopic fractionation values could not be estimated for control ii.a because the limited data points (n = 3) and extent of degradation (10 %) resulted in a statistically not significant regression ($p > 0.05$) (Figures C.2 and C.3). The isotopic findings align with the observed trends in reaction kinetics: the isotopic results for experiment ii.a (pH 11.4) are similar to those observed at pH 10.2 (experiments i.a and i.b) (Table 2), pointing to oxidation as the predominant degradation mechanism. Conversely, the isotopic data from experiment ii.b (pH 12.8) indicated a substantial contribution of AH in TCM degradation, as evidenced by εC and εCl values that fall within the range typically associated with AH. This result could thus explain the lower degradation rates observed in the vials at higher pH.

3.3. Experiment iii: impact of CO_3^{2-} on the radical cascade

In experiment iii, where CO_3^{2-} anion was introduced to the alkaline-activated PS system, the scavenging of $SO_4^{\cdot-}$ and $OH^{\cdot}$ radicals and the resulting generation of $CO_3^{\cdot-}$ radical anion was hypothesized based on previous studies [7,14]. TCM degradation reached 96 % after 20 days at pH 11.3 (iii.a) and 97 % after 67 days at pH 12.8 (iii.b). Estimated k'obs values were 0.16 ± 0.02 d^{-1} for experiment iii.a and 0.05 ± 0.01 d^{-1} for experiment iii.b (Figure C.1 and Table 2). At pH 11.3, the presence of CO_3^{2-} anion slightly enhanced TCM degradation kinetics ($t_{1/2} = 4.5$ days) compared to experiment ii.a ($t_{1/2} = 5.8$ days). However, the kinetics of experiments ii.b and iii.b were almost identical ($t_{1/2} = 13.1$ and 13.3 days, respectively), indicating that at pH 12.8, the degradation was mainly driven by AH, regardless of the presence of CO_3^{2-} anion.

Experiments iii.a and iii.b showed significant differences in isotopic fractionation (Figures C.2 and C.3), with εC values of -7.0 ± 0.6 ‰ and -26 ± 11 ‰, and εCl values of -0.5 ± 0.2 ‰ and -3.7 ± 0.3 ‰, respectively (Table 2). While the obtained $\Lambda^{C\text{-}Cl}$ values of 11 ± 5 and 10 ± 4 for these experiments could initially indicate an AH mechanism for both experiments, the differences observed in kinetics and isotopic fractionation values of C and Cl suggest that the presence of CO_3^{2-} anion might alter the TCM degradation mechanism at moderate alkaline pH (iii.a). The low εCl is similar to that observed in previous oxidative degradations (exp. i.a, i.b, iia), but the εC value is significantly lower. This difference may be related to the presence of different oxidative radicals, possibly $CO_3^{\cdot-}$. However, the contribution of superoxide anion radical ($O_2^{\cdot-}$) to TCM degradation cannot be discarded [47,48]. Considering this, the $\Lambda^{C\text{-}Cl}$ value observed in experiment iii.a might reflect

Table 2
Results of TCM degradation kinetics (k'obs and $t_{1/2}$), isotopic fractionation (εC and εCl) and dual C-Cl slope ($\Lambda^{C\text{-}Cl}$) for each experiment (Exp) and their corresponding controls without PS (below). Isotopic fractionation and dual isotope slope values are stated together with their ± 95 % confidence intervals. N = number of points; n.s. = not statistically significant ($p > 0.05$).

	Exp	pH	k'obs (d^{-1})	R^2	$t_{1/2}$ (d)	εC (‰)	εCl (‰)	$\Lambda^{C\text{-}Cl}$	N
Experimental	i.a	10.2 ± 0.2	0.15	0.939	4.6	−12 ± 1	−0.30 ± 0.05	33 ± 6	11
	i.b	10.2 ± 0.2	0.23	0.819	3.0	−11 ± 1	−0.4 ± 0.2	23 ± 10	10
	ii.a	11.4 ± 0.4	0.12	0.914	5.8	−10.1 ± 0.7	−0.4 ± 0.1	23 ± 7	7
	ii.b	12.8 ± 0.1	0.05	0.901	13.1	−25 ± 12	−2.7 ± 0.3	9 ± 2	6
	iii.a	11.3 ± 0.4	0.16	0.933	4.5	−7.0 ± 0.6	−0.5 ± 0.2	11 ± 5	7
	iii.b	12.8 ± 0.1	0.052	0.956	13.3	−26 ± 11	−3.7 ± 0.3	10 ± 4	5
	iv.a	10.6 ± 0.6	0.28	0.927	2.5	−3 ± 2	−0.6 ± 0.4	5.5 ± 0.6	4
Control	i.a	10.2 ± 0.2	0.001	0.008	802	n.s.	n.s.	n.s.	10
	i.b	10.2 ± 0.3	0.001	0.004	481	n.s.	n.s.	n.s.	10
	ii.a	11.4 ± 0.1	0.006	0.828	120	n.s.	n.s.	5 ± 3	3
	ii.b	12.8 ± 0.1	0.026	0.997	26.2	−59 ± 16	−5 ± 2	11 ± 1	4
	iv.a	11.6 ± 0.7	0.010	0.921	72.4	n.s.	n.s.	16 ± 15	4

mixed oxidative (as seen in experiment i.a, i.b and ii.a) and reductive degradation mechanisms. This hypothesis is further discussed in Section 3.6.

3.4. Experiment iv: mimicking alkaline trench conditions

In the PS experiments conducted under alkaline trench conditions (pH 10.6), containing trench-sampled solids and alkaline water, TCM degradation reached 99.9 % after 27 days (Figure C.1). In contrast, control vials without PS (pH 11.6) exhibited slower degradation kinetics, consuming only 27 % of TCM within the same time period. The estimated k'obs for the vials with PS was 0.28 ± 0.05 d^{-1}, with a half-life of 2.5 days, while the control vials showed values of 0.010 ± 0.002 d^{-1} and a half-life of 72.4 days (Table 2, Figure C.1). Notably, TCM degradation in the presence of PS under alkaline trench conditions exhibited the fastest kinetics among all the experiments performed.

Experimental vials exhibited significant shifts to higher $\delta^{13}C$ and $\delta^{37}Cl$ values of TCM, resulting in isotopic fractionation values of εC = -3 ± 2 ‰ (Figure C.2) and εCl = -0.6 ± 0.4 ‰ (Figure C.3), and a dual-element slope of 5.5 ± 0.6. In contrast, the control experiments yielded very different isotopic values; although εC and εCl could not be estimated because the linear regressions were not statistically significant ($p > 0.05$), a reliable $\Lambda^{C\text{-}Cl}$ value of 16 ± 6 was obtained.

These results indicate that in such a complex system, other processes may be influencing the removal of TCM in the control vials. One potential process is adsorption of organic compounds onto the solid phase, which may result in a reduction of the concentration of TCM without significantly changing its isotopic composition (see more details in Appendix E). In our study, the relatively high $\Lambda^{C\text{-}Cl}$ value obtained in the control experiments and the observed pH of 11.6 ± 0.7 are consistent with AH being the dominant process as already observed previously in similar conditions [28]. In addition, the AH process could be enhanced due to the equilibrium between the solid phase (containing concrete minerals such as portlandite, $Ca(OH)_2$) and the solution.

The experimental vials of experiment iv.a exhibited the lowest $\Lambda^{C\text{-}Cl}$ value (5.5 ± 0.6) among all the experiments, suggesting a minimal contribution of the AH mechanism, in agreement with the relatively moderate alkaline pH of 10.6. Similar $\Lambda^{C\text{-}Cl}$ values of 5.8 ± 0.4, 8 ± 2 and 6.7 ± 0.4 have been reported for abiotic reductive degradation of TCM by Fe(0) at neutral and alkaline pH [28,30] and by $CO_2^{\cdot-}$ radicals (via OS-SET), generated by thermal activation of PS and reaction with formate [35]. Although the initial CO_3^{2-} concentration in this experiment (95 mg/L) was similar to that in experiment iii.a (110 mg/L) (Table 2), the equilibrium with the solid phase in experiment iv.a resulted in a much higher final CO_3^{2-} concentration of approximately 300 mg/L. This suggests that there was sufficient CO_3^{2-} to scavenge hydroxide and sulphate radicals. In this scenario, superoxide radicals ($O_2^{\cdot-}$) might have contributed to TCM degradation, as ionic strength has been shown to enhance $O_2^{\cdot-}$ reactivity [8]. $O_2^{\cdot-}$ is known to act as both reducing and oxidizing agent [49]. In this case, given the low $\Lambda^{C\text{-}Cl}$ value determined for TCM in this experiment, $O_2^{\cdot-}$ radicals could drive TCM degradation primarily through a reductive mechanism. This suggest that the presence of PS and an excess of CO_3^{2-} could transform TCM degradation into an In Situ Chemical Reduction (ISCR) process rather than an ISCO. However, further evidence supporting this hypothesis is necessary.

Further insights into the potential reductive degradation of TCM were explored by comparing the results obtained for TCM with those for other CMs and CEs in experiments iv.a and iv.b, respectively (detailed in Appendix E). For CEs, PCE displayed low chlorine isotope fractionation (εCl = −0.4 ± 0.2) and a $\Lambda^{C\text{-}Cl}$ value of 5 ± 3 (Table E.1). This value is similar to the $\Lambda^{C\text{-}Cl}$ range of 4.6–7 reported for abiotically mediated RD by corrinoids [50], but diverge from those obtained for reduction of PCE, TCE and cis-DCE via OS-SET in experiments with $CO_2^{\cdot-}$ radical anion, which are reported to approach infinity because of the negligible chlorine isotopic fractionation [35]. In line with these discrepancies, TCE and cis-DCE in our experiments showed $\Lambda^{C\text{-}Cl}$ values of 6 ± 4 and 2 ± 1, respectively, contrasting with the trends for OS-SET.

The $\Lambda^{C\text{-}Cl}$ values for TCE (6 ± 4) and cis-DCE (2 ± 1) are relatively similar to the values reported for Fe(0)-induced (5.2 ± 0.3 for TCE and 3.1 ± 0.2 for cis-DCE, [51]) and corrinoids-induced (3.7–4.5 for TCE, [50]) reductive degradation. On the other hand, the isotopic fractionation results would also be consistent with those for CEs degradation with oxidation reactants. First, obtained εC value for TCE (-3.3 ± 0.4 ‰, Table E.1) is close to those reported for degradation with Fe(0)-activated PS at acid pH, both with (-3.4 to −4.3 ‰, [52]) and without (-3.9 to −4.7 ‰, [53]) carbonates, driven by $SO_4^{\cdot-}$ radical. Unfortunately, chlorine isotope data are not available for comparison. Second, the εC value for TCE is similar to that reported for Fenton-like degradation of TCE (-2.9 ± 0.3 ‰), where it was assumed that $OH^{\cdot}$ radical predominated and secondary chlorine isotopic fractionation resulted in a $\Lambda^{C\text{-}Cl}$ value of 3.1 ± 0.2 [54].

Overall, these results suggest that reductive processes could play a role in CEs degradation in the alkaline-activated PS system in presence of carbonates, and the observable chlorine isotopic fractionation tends to dismiss a stepwise OS-SET mechanism for CEs, in contrast to the observations with $CO_2^{\cdot-}$ radicals [35].

For the other CMs, for which limited isotopic data are available in the literature compared to TCM, CT exhibited a $\Lambda^{C\text{-}Cl}$ value of 2.2 ± 0.4 in experiment iv.a (Table E.1), closer to the value reported for magnetite ($Fe^{2+}Fe_2^{3+}O_4$)-mediated reductive reactions than to the one for Fe(0)-induced reaction (2 ± 1 and 5.8 ± 0.4, respectively) at pH 12 [29]. A potential reductive degradation of CT via reaction with $O_2^{\cdot-}$ could also be possible in our experiments. The reductive degradation of CT by $O_2^{\cdot-}$ radical anion was reported in previous studies [47,48], however, isotope data is still not available for this reaction. DCM, on the other hand, showed no statistically significant chlorine fractionation (with or without PS) and no $\Lambda^{C\text{-}Cl}$ values could thus be obtained (see Annex E).

3.5. Precipitate formation and chlorinated byproducts in experiments ii and iii

During experiments ii.a and iii.a (at pH 11.4 and 11.3, respectively), the formation of precipitate aggregates was observed in the vials containing PS (see figure F.1), but not in the control vials (Table F.1). HS-GC-qMS analysis identified and quantified higher chlorinated hydrocarbons alongside the degradation of TCM in the ii.a and iii.a experimental vials, while such byproducts were not detected in the control vials. This suggests that their formation is linked to the radical cascade in the oxidation process. Unexpectedly, the degradation of TCM in these conditions led thus to the accumulation of higher chlorinated compounds than the original contaminant, with hexachloroethane (HCA) emerging as the primary byproduct, and CT also detected. These compounds have been previously reported in photocatalytic degradation reactors of TCM and TCE [55,56], but, to the best of our knowledge, have never been associated with alkaline activated PS treatments.

The accumulation of HCA suggests that $OH^{\cdot}$ radicals, rather than $SO_4^{\cdot-}$ radicals, likely drove TCM degradation in experiments ii.a and iii.a, as prior findings have shown that $SO_4^{\cdot-}$ initiate HCA degradation [57], whereas HCA shows low reactivity with $OH^{\cdot}$ [48]. The formation of HCA might be explained by a HAA mechanism, where TCM reacts with $OH^{\cdot}$, similar to the mechanism proposed for 1,1,1-trichloroethane [58,59]. As a result, the C-H bond cleavage would produce trichloromethyl radicals ($CCl_3^{\cdot}$), which would subsequently dimerize to form HCA via radical coupling [60,61]. The formation of HCA occurs thus after the first reaction step of TCM degradation and, therefore, it does not influence the determined isotopic fractionation values of TCM. In experiment iv.a, although precipitates could not be observed because of the presence of the solid materials, HCA was also detected (Table F.1).

Due to the low solubility of HCA (50 mg/L) [62], it is likely that the observed precipitates corresponded to HCA. Direct quantification of precipitated HCA was challenging due to its volatility, which made

filtration, drying, and weighing unreliable. Therefore, an indirect calculation of the solid HCA formed during the experiments was performed using a chlorine mass balance equation (Eq. 3).

$$Cl_{TOT} = Cl^{-}_{aq} + Cl_{TCM} + Cl_{CT} + Cl_{HCA(aq)} + Cl_{HCA(s)} \quad (3)$$

Since the experiments were conducted in deionized water, the only initial source of chlorine was TCM (690 mg/L). Therefore, the total chlorine content in each experimental vial comprises the chloride anion present in the aqueous phase (Cl^{-}_{aq}, measured by HPLC), chlorine atoms in the dissolved organic chlorinated compounds (Cl_{TCM}, Cl_{CT} and $Cl_{HCA(aq)}$), and chlorine precipitated as solid HCA ($Cl_{HCA(s)}$). Results for estimated $Cl_{HCA(s)}$ are detailed in Table F.2. After near-complete transformation of TCM in experiments ii.a and iii.a, approximately 55–65 % of the initial chlorine from TCM was converted into HCA, predominantly recovered as precipitate (Fig. 1).

3.6. Insights into TCM degradation from 2D-CSIA

Isotope data revealed that while changes in TCM:PS molar ratio influence degradation kinetics they do not affect the degradation mechanism itself. Additionally, strong alkaline conditions (pH > 12) lead to the predominance of TCM degradation by AH over the reaction with PS-derived radical species, resulting in slower degradation kinetics. Consequently, isotope data from experiments for which differences between their dual element isotope trends were not significant ($p > 0.05$) were merged to derive combined $\Lambda^{C\text{-}Cl}$ values (i.e., experiments i.a + i.b + ii.a and experiments ii.b + iii.b). Obtained results are summarized in Fig. 2, where three distinct isotopic trends can be observed: (i) $\Lambda^{C\text{-}Cl}$ of 29 ± 4 during TCM oxidation by alkaline-activated PS (experiments i.a + i.b + ii.a). Compared to the slope from thermally activated PS (17 ± 2) [28], where $SO_4^{\cdot-}$ radicals are formed, the different slope obtained in this study suggest the involvement of $OH^{\cdot}$ radicals; (ii) $\Lambda^{C\text{-}Cl}$ between 11 ± 1 (Ctrl ii.b) and 9 ± 1 (experiments ii.b and iii.b), accompanied by significantly higher carbon and chlorine isotopic fractionation values for AH, where degradation predominantly follows the $E1_{CB}$ mechanism; and (iii) $\Lambda^{C\text{-}Cl}$ of 5.5 ± 0.6 during TCM degradation by alkaline-activated PS in experiments reproducing alkaline trench field conditions with the presence of excess of CO_3^{2-} (iv.a), which exhibited the fastest kinetics. The CO_3^{2-} anion can scavenge $SO_4^{\cdot-}$ and $OH^{\cdot}$ radical species and it could give rise to the contribution of other radical species, such as $O_2^{\cdot-}$, on TCM transformation. The reaction of TCM with $O_2^{\cdot-}$ could proceed via a reductive mechanism [47,48], however, the obtained slope differs from that reported for an OS-SET mechanism [35].

The observed C-Cl slope of experiment iii.a likely reflects a mixture of parallel or competing processes, suggesting the co-existence of oxidative-reductive reactions: oxidation (mainly via reaction with $OH^{\cdot}$) and a probable reductive reaction (driven by $O_2^{\cdot-}$), as suggested in experiment iv.a. An estimation of the contribution of each process to TCM degradation is shown in Appendix G, in the SI.

However, the range of $\Lambda^{C\text{-}Cl}$ values observed in our experiments also suggests that distinguishing between the action of alkaline-activated PS and TCM reductive biodegradation in the field may not always be possible based solely on isotopic C-Cl data. The range of $\Lambda^{C\text{-}Cl}$ values for RD of TCM (2.8 ± 0.3–7 ± 1, [33,31,32,34]) overlaps with the slope obtained in the presence of an excess of carbonates (exp. iv.a). In such cases, a more comprehensive analysis, including detailed hydrogeochemical and biological molecular tools, may be required to fully characterize the degradation mechanisms.

4. Conclusions

The degradation of TCM by alkaline-activated PS was studied in batch experiments to determine whether different factors such as TCM: PS molar ratio, pH and the presence of radical scavengers may affect the assessment of the degradation process by 2D-CSIA in ISCO treatments. In addition, experiments were performed reproducing alkaline trench field conditions to identify the factors driving the contaminant degradation processes in a complex field application scenario.

The distinct $\Lambda^{C\text{-}Cl}$ values obtained in this study provide compelling evidence of the potential of 2D-CSIA to differentiate between AH and other TCM degradation mechanisms, probably involving different ROS (e.g., $OH^{\cdot}$, $SO_4^{\cdot-}$, $O_2^{\cdot-}$ and $CO_3^{\cdot-}$), during alkaline-activated PS treatment in TCM-contaminated sites. These findings establish a solid foundation for understanding the multiple processes, that may occur simultaneously, during ISCO with alkaline-activated PS in contamination plumes. Further research using advanced techniques such as electron paramagnetic resonance (EPR) spectroscopy is needed to fully elucidate the specific radical species driving TCM degradation under the different conditions investigated.

The different carbon isotope fractionation values obtained in the experiments performed in this study underscore the need for caution when applying CSIA for the quantification of TCM degradation in the field. Relying on εC values obtained from simplified, deionized water experiments, common in literature, could lead to a significant underestimation of degradation extent when assessing TCM transformation with PS.

To the best of the authors' knowledge, this is the first study to document the formation of highly chlorinated byproducts such as HCA and CT during the chemical oxidation of TCM by PS. The formation of these byproducts raises important environmental concerns, as both HCA and CT are toxic and persistent in the environment. Several factors need to be considered when translating these findings to field applications: (i) our experiments were conducted in a closed system, leading to elevated byproducts concentrations that may be mitigated by dilution in natural

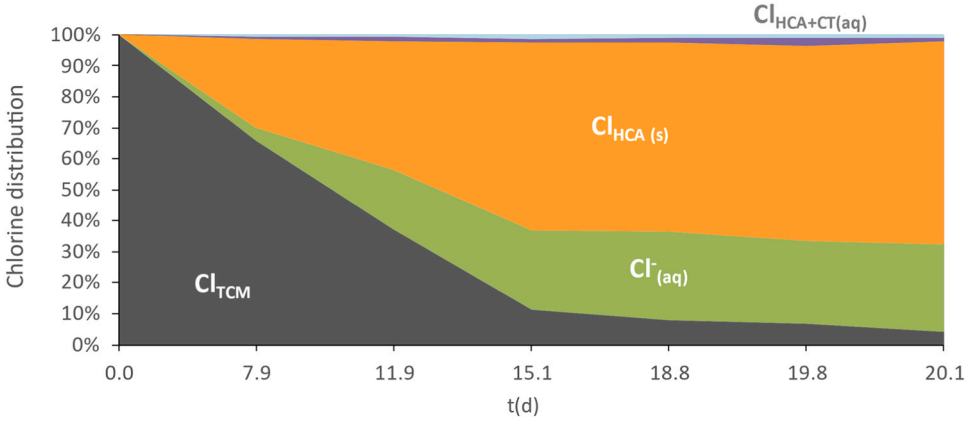

Fig. 1. Chlorine mass balance of experiment iii.a, showing quantified aqueous chloride and chlorine in dissolved TCM, CT and HCA, alongside the calculated chlorine precipitated as solid HCA.

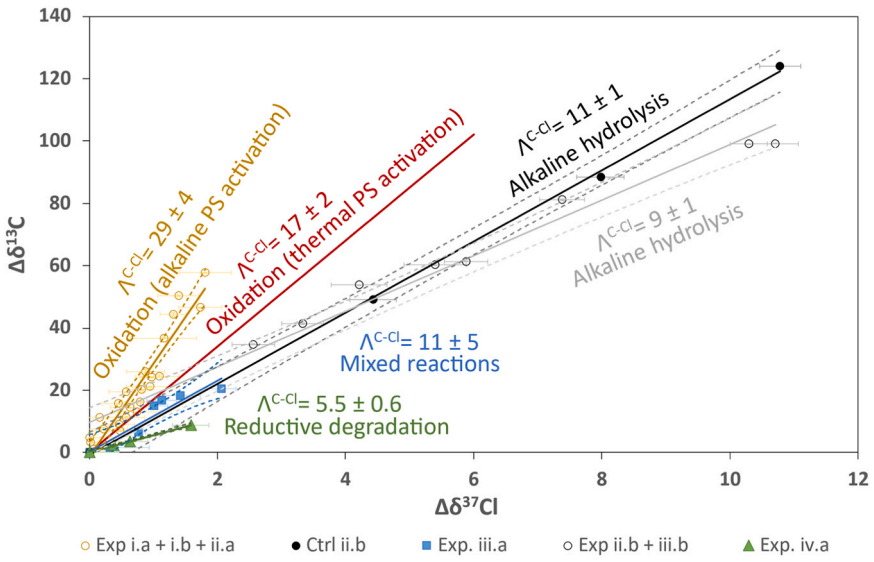

Fig. 2. Dual C-Cl isotope plot displaying results from different experiments with alkaline-activated PS (Exp) and control experiments without it (Ctrl), as well as the proposed TCM degradation mechanisms. Trends for thermally activated PS (in red) and alkaline hydrolysis ($\Lambda^{C\text{-}Cl}$ of 13.0 ± 0.8 at pH ~ 12, not shown) from [28] are shown for comparison. Data from some experiments was combined due to similarity ($p > 0.05$) (i.e., i.a + i.b + ii.a and ii.b + ii.b), yielding characteristic $\Lambda^{C\text{-}Cl}$ values. Dashed lines indicate the 95 % CI of the linear regression.

settings; (ii) the initial TCM concentration was 690 mg/L, which represents conditions near free-phase (DNAPL) zones or source areas of pollution, where PS treatments are often applied. Along the contamination plume, where the concentration of the contaminant is lower, expected generation of HCA would be reduced; (iii) processes such as volatilization and adsorption could reduce HCA concentrations in the field. Despite these considerations, the detection of HCA and CT in this study highlights the need for further investigation into the potential unintended consequences of PS-based ISCO techniques in TCM-contaminated sites. The results of this study might have thus important implications for the selection and evaluation of remediation strategies by decision-makers.

Environmental implications

TCM is one of the most prevalent contaminants in groundwater. ISCO using alkaline activated PS has gained increasing attention as a remediation method. This study demonstrates the potential of 2D-CSIA to differentiate between AH and other TCM degradation mechanisms, during alkaline-activated PS treatment in TCM-contaminated sites. Additionally, for the first time, hexachloroethane was observed as a byproduct of chloroform oxidation. These findings have important implications for the selection and evaluation of remediation strategies by decision-makers.

CRediT authorship contribution statement

Gil-Villalba Sergio: Writing – original draft, Visualization, Methodology, Investigation, Formal analysis, Data curation, Conceptualization. **Rosell Mònica:** Writing – review & editing, Visualization, Validation, Supervision, Methodology, Investigation, Formal analysis, Conceptualization. **Vinyes-Nadal Martí:** Writing – review & editing, Methodology, Investigation, Data curation, Conceptualization. **Torrentó Clara:** Writing – review & editing, Methodology, Investigation, Formal analysis, Conceptualization. **Palau Jordi:** Writing – review & editing, Validation, Supervision, Investigation, Conceptualization. **Soler Albert:** Validation, Supervision, Project administration, Methodology, Funding acquisition, Conceptualization.

Declaration of Competing Interest

The authors declare that they have no known competing financial interests or personal relationships that could have appeared to influence the work reported in this paper.

Acknowledgements

This study was financed through the following projects: PACE-ISOTEC (CGL2017–87216-C4–1-R) and REMECLOR (PDC2021–120861-C21), both funded by the Spanish Government and AEI/FEDER from the UE projects. This work was also supported by the Consolidate Research Group (2021SGR00308), funded by the AGAUR (Catalan Government). The experiments and work performed by S. Gil-Villalba were supported by the FPI2018/084979 contract. A small contribution for consumables was received from "Accions de Suport de l'Institut de Recerca de l'Aigua (IdRA) a la Recerca de Joves Investigadors" in 2021, 2022 and 2023. We thank all the technicians in MAiMA and CCiT-UB for their support. We thank two anonymous reviewers for their helpful comments that improved the quality of this manuscript.

Appendix A. Supporting information

Supplementary data associated with this article can be found in the online version at doi:10.1016/j.jhazmat.2025.137702.

Data availability

Data will be made available on request.

References

[1] ATSDR. (2023). *Substance Priority List [WWW Document]. Subst. Prior. List.* ⟨https://www.atsdr.cdc.gov/spl/index.html#2022spl⟩.
[2] Santos, A., Fernandez, J., Rodriguez, S., Dominguez, C.M., Lominchar, M.A., Lorenzo, D., Romero, A., 2018. Abatement of chlorinated compounds in groundwater contaminated by HCH wastes using ISCO with alkali activated persulfate. Sci Total Environ 615, 1070–1077. https://doi.org/10.1016/j.scitotenv.2017.09.224.
[3] Siegrist, R.L., Crimi, M., Brown, R.A., 2011. In: Siegrist, R.L., Crimi, M., Simpkin, T. J. (Eds.), In Situ Chemical Oxidation: Technology Description and Status BT - In Situ Chemical Oxidation for Groundwater Remediation. Springer New York, pp. 1–32. https://doi.org/10.1007/978-1-4419-7826-4_1.

[4] Tsitonaki, A., Petri, B., Crimi, M., Mosbk, H., Siegrist, R.L., Bjerg, P.L., 2010. In situ chemical oxidation of contaminated soil and groundwater using persulfate: a review. Crit Rev Environ Sci Technol 40 (1), 55–91. https://doi.org/10.1080/10643380802039303.
[5] Xu, J.C., Yang, L.H., Yuan, J.X., Li, S.Q., Peng, K.M., Lu, L.J., Huang, X.F., Liu, J., 2022. Coupling surfactants with ISCO for remediating of NAPLs: recent progress and application challenges. Chemosphere 303 (P1), 135004. https://doi.org/10.1016/j.chemosphere.2022.135004.
[6] Devi, P., Das, U., Dalai, A.K., 2016. In-situ chemical oxidation: principle and applications of peroxide and persulfate treatments in wastewater systems. Sci Total Environ 571, 643–657. https://doi.org/10.1016/j.scitotenv.2016.07.032.
[7] Li, W., Orozco, R., Camargos, N., Liu, H., 2017. Mechanisms on the impacts of alkalinity, pH, and chloride on persulfate-based groundwater remediation. Environ Sci Technol 51 (7), 3948–3959. https://doi.org/10.1021/acs.est.6b04849.
[8] Furman, O.S., Teel, A.L., Watts, R.J., 2010. Mechanism of base activation of persulfate. Environ Sci Technol 44 (16), 6423–6428. https://doi.org/10.1021/es1013714.
[9] Ike, I.A., Linden, K.G., Orbell, J.D., Duke, M., 2018. Critical review of the science and sustainability of persulphate advanced oxidation processes. Chem Eng J 338 (January), 651–669. https://doi.org/10.1016/j.cej.2018.01.034.
[10] Tian, K., Hu, L., Li, L., Zheng, Q., Xin, Y., Zhang, G., 2022. Recent advances in persulfate-based advanced oxidation processes for organic wastewater treatment. Chin Chem Lett 33 (10), 4461–4477. https://doi.org/10.1016/j.cclet.2021.12.042.
[11] Criquet, J., Leitner, N.K.V., 2009. Degradation of acetic acid with sulfate radical generated by persulfate ions photolysis. Chemosphere 77 (2), 194–200. https://doi.org/10.1016/j.chemosphere.2009.07.040.
[12] Furman, O.S., Teel, A.L., Ahmad, M., Merker, M.C., Watts, R.J., 2011. Effect of basicity on persulfate reactivity. J Environ Eng 137 (4), 241–247. https://doi.org/10.1061/(asce)ee.1943-7870.0000323.
[13] Liang, C., Lei, J., 2015. Identification of active radical species in alkaline persulfate oxidation. Water Environ Res 87 (7), 656–659. https://doi.org/10.2175/106143015x14338845154986.
[14] Lee, J., Von Gunten, U., Kim, J.H., 2020. Persulfate-based advanced oxidation: critical assessment of opportunities and roadblocks. Environ Sci Technol 54 (6), 3064–3081. https://doi.org/10.1021/acs.est.9b07082.
[15] Qi, C., Liu, X., Ma, J., Lin, C., Li, X., Zhang, H., 2016. Activation of peroxymonosulfate by base: Implications for the degradation of organic pollutants. Chemosphere 151, 280–288. https://doi.org/10.1016/j.chemosphere.2016.02.089.
[16] Ma, J., Yang, Y., Jiang, X., Xie, Z., Li, X., Chen, C., Chen, H., 2018. Impacts of inorganic anions and natural organic matter on thermally activated persulfate oxidation of BTEX in water. Chemosphere 190, 296–306. https://doi.org/10.1016/j.chemosphere.2017.09.148.
[17] Nie, M., Yang, Y., Zhang, Z., Yan, C., Wang, X., Li, H., Dong, W., 2014. Degradation of chloramphenicol by thermally activated persulfate in aqueous solution. Chem Eng J 246, 373–382. https://doi.org/10.1016/j.cej.2014.02.047.
[18] Buxton, G.V., Greenstock, C.L., Helman, W.P., Ross, A.B., 1988. Critical review of rate constants for reactions of hydrated electrons, hydrogen atoms and hydroxyl radicals (·OH/·O− in aqueous solution. J Phys Chem Ref Data 17 (2), 513–886. https://doi.org/10.1063/1.555805.
[19] Ji, Y., Wang, L., Jiang, M., Lu, J., Ferronato, C., Chovelon, J.M., 2017. The role of nitrite in sulfate radical-based degradation of phenolic compounds: an unexpected nitration process relevant to groundwater remediation by in-situ chemical oxidation (ISCO). Water Res 123, 249–257. https://doi.org/10.1016/j.watres.2017.06.081.
[20] Lian, L., Yao, B., Hou, S., Fang, J., Yan, S., Song, W., 2017. Kinetic study of hydroxyl and sulfate radical-mediated oxidation of pharmaceuticals in wastewater effluents. Environ Sci Technol 51 (5), 2954–2962. https://doi.org/10.1021/acs.est.6b05536.
[21] Canonica, S., Kohn, T., Mac, M., Real, F.J., Wirz, J., Von Gunten, U., 2005. Photosensitizer method to determine rate constants for the reaction of carbonate radical with organic compounds. Environ Sci Technol 39 (23), 9182–9188. https://doi.org/10.1021/es051236b.
[22] Liu, Y., Zhang, Y., Zhou, A., Li, M., 2021. Insights into carbon isotope fractionation on trichloroethene degradation in base activated persulfate process: the role of multiple reactive oxygen species. Sci Total Environ 800, 149371. https://doi.org/10.1016/j.scitotenv.2021.149371.
[23] Torrentó, C., Audí-Miró, C., Bordeleau, G., Marchesi, M., Rosell, M., Otero, N., Soler, A., 2014. The use of alkaline hydrolysis as a novel strategy for chloroform remediation: the feasibility of using construction wastes and evaluation of carbon isotopic fractionation. Environ Sci Technol 48 (3), 1869–1877. https://doi.org/10.1021/es403838t.
[24] Elsner, M., 2010. Stable isotope fractionation to investigate natural transformation mechanisms of organic contaminants: principles, prospects and limitations. J Environ Monit 12 (11), 2005–2031. https://doi.org/10.1039/c0em00277a.
[25] Lincker, M., Lagneau, V., Guillon, S., Wanner, P., 2022. Identification of chlorohydrocarbon degradation pathways in aquitards using dual element compound-specific isotope measurements in aquifers. Chemosphere 303 (P2), 135131. https://doi.org/10.1016/j.chemosphere.2022.135131.
[26] Palau, J., Jamin, P., Badin, A., Vanhecke, N., Haerens, B., Brouyère, S., Hunkeler, D., 2016. Use of dual carbon-chlorine isotope analysis to assess the degradation pathways of 1,1,1-trichloroethane in groundwater. Water Res 92, 235–243. https://doi.org/10.1016/j.watres.2016.01.057.
[27] Wiegert, C., Aeppli, C., Knowles, T., Holmstrand, H., Evershed, R., Pancost, R.D., Macháčková, J., Gustafsson, Ö., 2012. Dual carbon-chlorine stable isotope investigation of sources and fate of chlorinated ethenes in contaminated groundwater. Environ Sci Technol 46 (20), 10918–10925. https://doi.org/10.1021/es3016843.
[28] Torrentó, C., Palau, J., Rodríguez-Fernández, D., Heckel, B., Meyer, A., Domènech, C., Rosell, M., Soler, A., Elsner, M., Hunkeler, D., 2017. Carbon and chlorine isotope fractionation patterns associated with different engineered chloroform transformation reactions. Environ Sci Technol 51 (11), 6174–6184. https://doi.org/10.1021/acs.est.7b00679.
[29] Rodríguez-Fernández, D., Heckel, B., Torrentó, C., Meyer, A., Elsner, M., Hunkeler, D., Soler, A., Rosell, M., Domènech, C., 2018. Dual element (C-Cl) isotope approach to distinguish abiotic reactions of chlorinated methanes by Fe(0) and by Fe(II) on iron minerals at neutral and alkaline pH. Chemosphere 206, 447–456. https://doi.org/10.1016/j.chemosphere.2018.05.036.
[30] Asfaw, B.A., Sakaguchi-Söder, K., Schiedek, T., Michelsen, N., Bernstein, A., Siebner, H., Schüth, C., 2023. Isotopic evidence (δ13C, δ37Cl, δ2H) for distinct transformation mechanisms of chloroform: catalyzed H2-water system vs. zero-valent iron (ZVI). J Environ Chem Eng 11 (3). https://doi.org/10.1016/j.jece.2023.110005.
[31] Heckel, B., Phillips, E., Edwards, E., Sherwood Lollar, B., Elsner, M., Manefield, M. J., Lee, M., 2019. Reductive dehalogenation of trichloromethane by two different dehalobacter restrictus strains reveal opposing dual element isotope effects. Environ Sci Technol 53 (5), 2332–2343. https://doi.org/10.1021/acs.est.8b03717.
[32] Rodríguez-Fernández, D., Torrentó, C., Guivernau, M., Viñas, M., Hunkeler, D., Soler, A., Domènech, C., Rosell, M., 2018. Vitamin B12 effects on chlorinated methanes-degrading microcosms: dual isotope and metabolically active microbial populations assessment. Sci Total Environ 621, 1615–1625. https://doi.org/10.1016/j.scitotenv.2017.10.067.
[33] Heckel, B., Elsner, M., 2022. Exploring mechanisms of biotic chlorinated alkane reduction: evidence of nucleophilic substitution (SN2) with vitamin B12. Environ Sci Technol 56 (10), 6325–6336. https://doi.org/10.1021/acs.est.1c06066.
[34] Soder-Walz, J.M., Torrentó, C., Algora, C., Wasmund, K., Cortés, P., Soler, A., Vicent, T., Rosell, M., Marco-Urrea, E., 2022. Trichloromethane dechlorination by a novel Dehalobacter sp. strain 8M reveals a third contrasting C and Cl isotope fractionation pattern within this genus. Sci Total Environ 813. https://doi.org/10.1016/j.scitotenv.2021.152659.
[35] Heckel, B., Cretnik, S., Kliegman, S., Shouakar-Stash, O., McNeill, K., Elsner, M., 2017. Reductive outer-sphere single electron transfer is an exception rather than the rule in natural and engineered chlorinated ethene dehalogenation. Environ Sci Technol 51 (17), 9663–9673. https://doi.org/10.1021/acs.est.7b01447.
[36] Huling, S.G., Ko, S., Pivetz, B., 2011. Groundwater sampling at ISCO sites: binary mixtures of volatile organic compounds and persulfate. Ground Water Monit Remediat 31 (2), 72–79. https://doi.org/10.1111/j.1745-6592.2011.01332.x.
[37] Cao, M., Hou, Y., Zhang, E., Tu, S., Xiong, S., 2019. Ascorbic acid induced activation of persulfate for pentachlorophenol degradation. Chemosphere 229, 200–205. https://doi.org/10.1016/j.chemosphere.2019.04.135.
[38] Jin, B., Laskov, C., Rolle, M., Haderlein, S.B., 2011. Chlorine isotope analysis of organic contaminants using GC-qMS: method optimization and comparison of different evaluation schemes. Environ Sci Technol 45 (12), 5279–5286. https://doi.org/10.1021/es200749d.
[39] Shouakar-Stash, O., Drimmie, R.J., Zhang, M., Frape, S.K., 2006. Compound-specific chlorine isotope ratios of TCE, PCE and DCE isomers by direct injection using CF-IRMS. Appl Geochem 21 (5), 766–781. https://doi.org/10.1016/j.apgeochem.2006.02.006.
[40] Coplen, T.B., 1996. New guidelines for reporting stable hydrogen, carbon, and oxygen isotope-ratio data. Geochim Et Cosmochim Acta 60 (17), 3359–3360. https://doi.org/10.1016/0016-7037(96)00263-3.
[41] Kaufmann, R., Long, A., Bentley, H., Davis, S., 1984. Natural chlorine isotope variations. Nature 309 (5966), 338–340. https://doi.org/10.1038/309338a0.
[42] Coplen, T.B., 2011. Guidelines and recommended terms for expression of stable-isotope-ratio and gas-ratio measurement results. Rapid Commun Mass Spectrom 25 (17), 2538–2560. https://doi.org/10.1002/rcm.5129.
[43] Elsner, M., Hunkeler, D., 2008. Evaluating chlorine isotope effects from isotope ratios and mass spectra of polychlorinated molecules. Anal Chem 80 (12), 4731–4740. https://doi.org/10.1021/ac702543y.
[44] Ojeda, A.S., Phillips, E., Mancini, S.A., Lollar, B.S., 2019. Sources of uncertainty in biotransformation mechanistic interpretations and remediation studies using CSIA. Anal Chem 91 (14), 9147–9153. https://doi.org/10.1021/acs.analchem.9b01756.
[45] Ojeda, A.S., Phillips, E., Sherwood Lollar, B., 2020. Multi-element (C, H, Cl, Br) stable isotope fractionation as a tool to investigate transformation processes for halogenated hydrocarbons. Environ Sci: Process Impacts 22 (3), 567–582. https://doi.org/10.1039/C9EM00498J.
[46] Liang, C., Su, H.W., 2009. Identification of sulfate and hydroxyl radicals in thermally activated persulfate. Ind Eng Chem Res 48 (11), 5558–5562. https://doi.org/10.1021/ie9002848.
[47] Smith, B.A., Teel, A.L., Watts, R.J., 2006. Mechanism for the destruction of carbon tetrachloride and chloroform DNAPLs by modified Fenton's reagent. J Contam Hydrol 85 (3–4). https://doi.org/10.1016/j.jconhyd.2006.02.002.
[48] Teel, A.L., Watts, R.J., 2002. Degradation of carbon tetrachloride by modified Fenton's reagent. J Hazard Mater 94 (2), 179–189. https://doi.org/10.1016/S0304-3894(02)00068-7.
[49] Watts, R.J., Bottenberg, B.C., Hess, T.F., Jensen, M.D., Teel, A.L., 1999. Role of reductants in the enhanced desorption and transformation of chloroaliphatic compounds by modified Fenton's reactions. Environ Sci Technol 33 (19). https://doi.org/10.1021/es990054c.
[50] Renpenning, J., Keller, S., Cretnik, S., Shouakar-Stash, O., Elsner, M., Schubert, T., Nijenhuis, I., 2014. Combined C and Cl isotope effects indicate differences between corrinoids and enzyme (Sulfurospirillum multivorans PceA) in reductive

dehalogenation of tetrachloroethene, but not trichloroethene. Environ Sci Technol 48 (20), 11837–11845. https://doi.org/10.1021/es503306g.
[51] Audí-Miró, C., Cretnik, S., Otero, N., Palau, J., Shouakar-Stash, O., Soler, A., Elsner, M., 2013. Cl and C isotope analysis to assess the effectiveness of chlorinated ethene degradation by zero-valent iron: evidence from dual element and product isotope values. Appl Geochem 32, 175–183. https://doi.org/10.1016/j.apgeochem.2012.08.025.
[52] Liu, Y., Zhou, A., Gan, Y., Li, X., 2016. Variability in carbon isotope fractionation of trichloroethene during degradation by persulfate activated with zero-valent iron: Effects of inorganic anions. Sci Total Environ *548–549*. https://doi.org/10.1016/j.scitotenv.2016.01.011.
[53] Liu, Y., Zhou, A., Gan, Y., Li, X., 2018. Roles of hydroxyl and sulfate radicals in degradation of trichloroethene by persulfate activated with Fe2+ and zero-valent iron: Insights from carbon isotope fractionation. J Hazard Mater 344, 98–103. https://doi.org/10.1016/j.jhazmat.2017.09.048.
[54] Liu, Y., Gan, Y., Zhou, A., Liu, C., Li, X., Yu, T., 2014. Carbon and chlorine isotope fractionation during Fenton-like degradation of trichloroethene. Chemosphere 107, 94–100. https://doi.org/10.1016/j.chemosphere.2014.03.011.
[55] Cohen, L.R., Peña, L.A., Seidl, A.J., Chau, K.N., Keck, B.C., Feng, P.L., Hoggard, P. E., 2009. Photocatalytic degradation of chloroform by bis (bipyridine) dichlororuthenium(III/II). J Coord Chem 62 (11), 1743–1753. https://doi.org/10.1080/00958970802702254.
[56] Hung, C.-H., MariÑas, B.J., 1997. Role of chlorine and oxygen in the photocatalytic degradation of trichloroethylene vapor on TiO2 films. Environ Sci Technol 31 (2), 562–568. https://doi.org/10.1021/es960465i.
[57] Zhu, C., Zhu, F., Liu, C., Chen, N., Zhou, D., Fang, G., Gao, J., 2018. Reductive hexachloroethane degradation by S2O8•- with thermal activation of persulfate under anaerobic conditions. Environ Sci Technol 52 (15), 8548–8557. https://doi.org/10.1021/acs.est.7b06279.
[58] Gu, X., Lu, S., Li, L., Qiu, Z., Sui, Q., Lin, K., Luo, Q., 2011. Oxidation of 1,1,1-trichloroethane stimulated by thermally activated persulfate. Ind Eng Chem Res 50 (19). https://doi.org/10.1021/ie201059x.
[59] Palau, J., Shouakar-Stash, O., Hunkeler, D., 2014. Carbon and chlorine isotope analysis to identify abiotic degradation pathways of 1,1,1-trichloroethane. Environ Sci Technol 48 (24). https://doi.org/10.1021/es504252z.
[60] Rodríguez-Chueca, J., Mediano, A., Pueyo, N., García-Suescun, I., Mosteo, R., Ormad, M.P., 2016. Degradation of chloroform by Fenton-like treatment induced by electromagnetic fields: a case of study. Chem Eng Sci 156. https://doi.org/10.1016/j.ces.2016.09.016.
[61] Tang, W.Z., Tassos, S., 1997. Oxidation kinetics and mechanisms of trihalomethanes by Fenton's reagent. Water Res 31 (5). https://doi.org/10.1016/S0043-1354(96)00348-X.
[62] Horvath, A.L., Getzen, F.W., Maczynska, Z., 1999. IUPAC-NIST solubility data series 67. Halogenated ethanes and ethenes with water. J Phys Chem Ref Data 28 (2), 395–627. https://doi.org/10.1063/1.556039.